REVIEW

Conversion reactions: a new pathway to realise energy in lithium-ion battery—review

R. Malini · U. Uma · T. Sheela · M. Ganesan · N. G. Renganathan

Abstract Rechargeable lithium-ion batteries of today operate by an electrochemical process that involves intercalation reactions that warrants the use of electrode materials having very specific structures and properties. Further, they are limited to the insertion of one Li per 3D metal. One way to circumvent this intrinsic limitation and achieve higher capacities would be the use of electrode materials in which the metal-redox oxidation state could reversibly change by more than one unit. Through the discovery of conversion or displacement reactions, it is possible to reversibly change by more than one unit. Further, the need for materials with open structures or good electronic ionic conductivity is eliminated, thus leading to a new area in materials for lithium ion battery. In this paper, we present a review enlightens new reaction schemes and their potential impact on applications.

Keywords Anode · Lithium-ion battery · Conversion reaction · Intercalation/de-intercalation

Introduction

Lithium ion batteries are the key components of portable electronics in the present information-rich mobile society. The present Li-ion battery uses the swing action of lithium ion between positive $LiCoO_2$ electrode and negative carbon electrode (insertion/de-insertion process). The problems like low discharge rate capability of graphite, safety, life spans being limited by Li-alloying agglomeration, and growth of passivation layers restrict the full utilization of reversible insertion/de-insertion process. Structural change of the host occurs during charge and discharge processes, minimizing the continued reversibility of the redox processes. As a result, the reaction is restricted to single electron transfer. This limits the volumetric and gravimetric energy density that can be achieved with Li-ion batteries. Driven by EV market demands, namely in terms of volume restriction, researchers have focused their attention on the search for either (1) high-voltage redox systems (e.g., highly oxidant positive electrode materials) so that fewer cells will be required for a predefined application voltage or (2) high-energy density systems by increasing the volumetric capacity of either the positive or negative electrode to reduce the size of each cell and, therefore, of the overall stack [1].

With the existing technology, high rate, quick-charging Li-ion battery is not possible. Deviating from the usual macro-level chemistry, the nanoscale materials offer the promising alternative electrode material with its remarkable properties. Hence, it is felt that to emphasize through this short review the need for future battery, we report the various electrode materials which exploit the conversion reaction where intercalation combined with Faradaic reaction will be the main reactions wherein high energy is expected to attain.
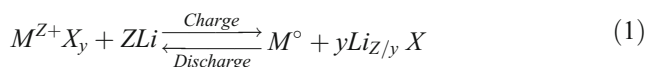
Conversion reactions

Conversion reactions are those in which an active electrode material, MX_y, is consumed by Li and reduced to the metal
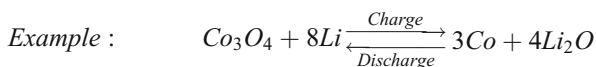
R. Malini · U. Uma · T. Sheela
Centre for Education, Central Electrochemical Research Institute,
Karaikudi 630 006, India

M. Ganesan (✉) · N. G. Renganathan
Electrochemical Energy systems Division,
Central Electrochemical Research Institute,
Karaikudi 630 006, India
e-mail: mgshan2002@yahoo.co.in

M and a corresponding lithium compound, according to the general reaction:

$$M^{Z+}X_y + ZLi \xrightleftharpoons[\text{Discharge}]{\text{Charge}} M^\circ + yLi_{Z/y}X \qquad (1)$$

where M represents the cation and X, the anion

$$Example: \qquad Co_3O_4 + 8Li \xrightleftharpoons[\text{Discharge}]{\text{Charge}} 3Co + 4Li_2O$$

The fundamental route to attain the highest specific capacity of an electrode is to utilize all the possible oxidation states of a compound during the redox cycle. In general, an increase in the Me–X bond ionicity results in an increase in the output voltage associated with reaction 1. Therefore, the output voltage of reaction 1 would expect to increase through the highly covalent metal nitrides and sulfides, to the metal oxides, through the inductive effect polyanions (metal phosphates, metal borates), and finally to the highly ionic metal fluoride [2] (Fig. 1).

The matrix ensures good electronic conductivity, while the fine nanoscale nature (30nm or less) of metal nanocomposite minimizes Li^+ diffusion distance. As a result, technologically important properties such as large specific capacities, sustained reversibility, and large capacity at low potential have been demonstrated in these compounds. In conversion reaction, more than one electron transfer occurs per 3D metal, while in the intercalation process, it is limited to $0.5e^-$ transfer.

One of the advantages of nanostructured materials in preference to nanoscale materials is their potential to deliver superior rate capability, i.e., fast charge/discharge. As the main advantage of employing conversion reactions is their superior capacity compared with intercalation electrodes, it is necessary to investigate the rate capability of such conversion reactions over a wide composition (voltage) range.

Another attractive aspect is that the potential of these conversion reactions depends on the ionic valence of the M–X bonding and therefore can be tuned into a continuous

Fig. 1 Conversion mechanism in Co_3O_4 (courtesy of Hu et al. [4])

line from 0 to 3V by changing the nature of the anion X, with the highest potential obtained for fluorides.

To fully harvest the potentials of conversion reaction, one needs to address the problems like (1) poor kinetics that result in a large polarization, and hence a poor energy efficiency, (2) poor capacity retention upon cycling, (3) higher potentials, and hence a lower cell voltage unless coupled with a higher voltage electrode, (4) irreversible capacity loss on the first cycle, poor rate, (5) poor capacity retention on cycling, (6) find chemical ways to lower and narrow their voltage reactivity range toward Li, (7) marked hysteresis in voltage between charge and discharge, and (8) low coulombic efficiency. These limit the energy efficiency and power capabilities of batteries using conversion reactions. The low coulombic efficiency can be attributed to a variety of shortcomings, for example, irreversible trapping of lithium ions in host materials, interference with the organic electrolyte (solid electrolyte interphase), or the loss of electrical contact of the electrode material with the current collector. This reduces the energy densities of Li ion battery and is a serious trade-off in battery technology.

In the full literature survey of materials right from metal fluorides, sulfides, antimonides, stannides, oxides, and phosphides, the polarization, ϕV, is decreasing as we move from fluorides ($\Phi V \approx 1.1$V) to oxides ($\Phi V \approx 0.9$V), sulfides ($\Phi V \approx 0.7$V), and phoshides ($\Phi V \approx 0.4$V). This is fully consistent with the decrease in the M–X bond polarization from M–F to M–P [1].

Kinetic improvements in conversion reactions, together with an enhancement of their capacity retention, were achieved by either (1) acting at the particle surfaces through the use of conducting coatings as reported by Hu et al. [4] for carbon-coated Cr_2O_3 particles, (2) moving from bulk to thin-film material as illustrated by the studies by Pralong et al. [5] on Co_3O_4 thin films, or (3) playing with new nanostructured electrode design.

Tarascon et al. reported on a new electrode configuration that consists of the high temperature growth of an electrochemical oxide layer at the surface of a stainless steel current collector. Owing to this chemically made current collector/active material interface, the electrode shows an outstanding capacity retention even after >800 cycles and good kinetics (90% of the full capacity at 1C). Therefore, such electrodes still suffer from a large polarization (~0.8V) that is intrinsic to conversion reactions and linked, among others, to the electrical energy needed to overcome the energetic barrier. The latter is associated to the reversible breaking/formation of chemical M–X bonds as well as to the electronic and ionic conducting properties of the precursors M_xX_y and generated Li-based ternary phases [6, 7].

In 2006, Tarascon et al. reported a simple, two-step Fe_3O_4 electrode fabrication process that consists of growing

a 3D array of copper nanorods onto the copper foil by electrodeposition through a porous anodic alumina membrane that is subsequently dissolved followed by the electrodeposition of magnetite by cathodic reduction of a Fe(III) chelate precursor in alkaline solution [8].

An appropriate anode material should exhibit low voltage, while a cathode material should exhibit a high voltage vs. Li^+/Li.

Negative electrode materials for conversion reactions

With respect to negative electrode materials, metal alloys or intermetallic compounds are attractive alternatives to graphite because they can be selected to operate between 0 and 1V above the potential of metallic lithium. Many intermetallic compounds, Li_xM (e.g., Sb, Al, Sn, Si), have already been investigated. But the metals possess very dense structures, so reactions with lithium tend to be accompanied by large changes in volume and by major structural rearrangements. The severe crystallographic changes that occur during charge and discharge of the cells lead to mechanical disintegration of the intermetallic structures, insulating layers on the surface of the electrochemically pulverized electrode particles and a loss of electronic particle-to-particle contact. These effects seriously affect the cycling efficiency and cycle life of lithium cells. However, when reduced to nanoscale, reversible conversion reactions occur. Explorations of transition metal oxides as negative electrode materials, first reported by Idota et al. [1], Tarascon et al. [2], and Leroux et al. [3], were pursued and led to the development of new concepts regarding Li uptake/removal mechanism. Recent interest has also been aroused by reports on Li uptake in transition metal compounds of Group V, such as phosphides (CoP_3) and antimonides ($CoSb_3$), which show a similar reversible Li uptake [4, 5]. It was shown that as well as the reduction of metal oxide with lithium, besides the growth of metal nanoparticles and Li_2O or Li_3P, Li_3Sb, there was also the formation of a polymeric interface growth between the active material and the electrolyte.

Oxides

Poizot et al. reported the reversible electrochemical activity of nano-sized transition metal oxides with lithium with 100% capacity retention up to 100 cycles [9]. The mechanism of Li reactivity in such materials differs from the classical processes and is nested in the electrochemically driven in situ formation of metal nanoparticles during the first discharge, which enables the formation and decomposition of Li_2O upon subsequent cycling. The reversible electrochemical reaction mechanism of Li with the TMO

entails for most part of the displacement redox reaction called as conversion reaction [9].

Furthermore, for conversion reaction (CoO, Fe_2O_3, Co_3O_4…), the amazing reactivity of these oxides has been linked to the O^{2-} ion mobility within the Li_2O/metallic particle nanocomposite formed. Instead of conventional powder material, electrode material is taken in the form of thin films prepared by radio frequency sputtering, laser ablation, or pulsed laser deposition, nanowires, nanoflakes, and mesoporous structures using the hard templates like SBA-15 (1D pore structure) and KIT-6 (3D pore structure) [10–15].

The intercalated phase is always formed upon reduction of Co_3O_4, and its stability is highly dependent on the applied current density. When the current density is high enough, $Li_xCo_3O_4$ remains stable, and its growth is therefore observed, although it spontaneously decomposes into CoO when this current density is reduced or interrupted intermittently.

The formation of the intercalated lithiated phase is governed by the current density (A/m^2) at the surface of the particles and favored by a high current density. When the intercalated phase is not detected, CoO presently appears to be the intermediate between Co_3O_4 and metallic cobalt. The nature of the intermediate is thus rate/surface-dependent. This mechanism is consistent with the observations made by Thackeray et al. [17] regarding the necessity of using fast chemical reduction instead of slow electrochemical reduction to be able to observe a $Li_xCo_3O_4$ phase by X-ray.

In Fig. 2, the formation of intercalated $Li_xCo_3O_4$ (pathway 1) competes with the departure of oxygen from the spinel framework (pathway 2), the favored path being driven by the current density.

The factors affecting the reduction path of Co_3O_4 are the texture of the active material such as specific surface area and crystallite size and the cycling procedure such as rate and temperature. The confinement of the metallic clusters in an amorphous matrix can account for the integrity of the reactive particles and the absence of internal loss of electrical contact.

The behavior of the nanowires and nanoparticles is, however, significantly different from the mesoporous material. All three nanomaterials of Co_3O_4 show a marked increase in capacity on initial cycling, up to 10–15 cycles. The capacities exceed the theoretical value for the conversion reaction, indicating that the excess capacity is associated with increased charge storage within the polymeric surface
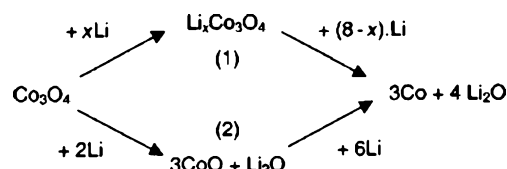

Fig. 2 Conversion reaction in Co_3O_4 (courtesy of Larcehr et al. [16])

layer [18, 19]. The higher surface areas of the nanomaterials permits, on cycling, an increase in the extent of polymer layer formation per unit mass of electrode material.

As the mesoporous material enhances the access of Li^+ in the electrolyte to the Co_3O_4 surface and the thin walls aid ion transport as well as better accommodating volume changes encountered with the two phase reaction (i.e., reducing strain), one might have anticipated better rate capability. The lack of improvement paths to the electron transport within the particles is the rate-limiting step [20].

Comparing nano, mesoporous, and micrometer α-Fe_2O_3, the first two enhance Li^+ transport to (high surface area) and within the particles/walls as well as ease the strain of the conversion reaction; however, mesoporous α-Fe_2O_3 does not enhance e− transport (micrometer particle size), demonstrating the importance of e− transport within the particles in achieving high rates [21]. Balaya et al. have shown that for conversion reactions involving metal oxides that are good electronic conductors (specifically RuO_2), the irreversible capacity on the first cycle can be reduced significantly [22, 23].

Although the Li storage is complex in RuO_2, through the homogeneous formation of $LiRuO_2$ followed by the heterogeneous formation of Ru/Li_2O and a Li-containing SEI film, in addition to the interfacial deposition within the Ru/Li_2O nanocomposite, these processes can still be highly reversible with more than 98% coulombic efficiency and retain a capacity of 1,110mAh/g in the voltage range of 0.05–4.3V and 99% coulombic efficiency with a capacity of 730mAh/g at 0.8–4.3V. This is at least partly due to the high electronic and ionic conductivity in addition to the formation of a kinetically favored nanostructure (2–5nm) [24].

The Cr_2O_3 reacts towards Li through a conversion reaction mechanism leading, upon discharge, to the formation of large metallic chromium nanoparticles (10nm); the latter are embedded into a Li_2O matrix together with, in this specific case, a copious amount of polymeric materials coming from electrolyte degradation surrounding the particles and filling the pores [25]. During the following charge, re-oxidation of the nanoparticles occurs with the formation of CrO_{1-x}, with the main difference, as opposed to bulk Cr_2O_3 electrodes, being the preservation of the polymeric layer at the end of the charge. These electrolyte degradation products are shown to help in maintaining the material mesoporosity for a great number of cycles, and, interestingly, they are not detrimental to the cell performance in terms of capacity retention while presenting great advantages in terms of charge transfer by reducing diffusion lengths, namely for Li^+ ions.

An evident advantage of mesoporous chromium oxide lies in (1) the grain size shortening, which enables a better fuelling of the electrons into the electrode, although CrO is a poor electronic conductor [26] and (2) the specific material morphology that decreases the diffusion path for ions and enhances the access of cation in the electrolyte. Such better electronic/ionic wiring of the electrode also accounts for the decrease in polarization observed for the mesoporous electrode.

Fluorides

Metal fluorides have been largely ignored as reversible positive electrodes for rechargeable lithium batteries. This is due to their insulative nature brought about by their characteristic large band gap. To exploit the electrochemical activity of metal fluorides, there are two ways: (1) drastic reduction of crystal size by high energy milling and (2) use of highly conducting carbon to electrically connect the grains of metal fluoride molecule.

The structure and electrochemistry of FeF_3:C-based carbon metal fluoride nanocomposites (CMFNCs) was investigated by Amatucci et al. from 4.5 to 1.5V, revealing a reversible metal fluoride conversion process. A reversible specific capacity of approximately 600mAh/g of CMFNCs was realized at 70°C. The potentials utilized during the anodic reaction are much higher than the analogous oxide reaction. They exceed the values to oxidize the Fe into the solution of the electrolyte. At this early stage, the high capacities (600mAh/g) of the fluorides are only accessible at elevated temperature and/or low rate [27].
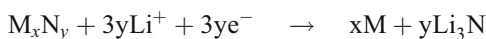
LiF is electrochemically active in the form of M/LiF composites in which amorphous LiF and metal are dispersed on an atomic or a nanometer scale. Such composites are obtained by a complete but heterogeneous electrochemical insertion of Li into the transition metal fluorides. Consequently, the formation and decomposition of LiF can be obtained at room temperature. The reversible Li storage capacities of TiF3 and VF3 are as high as 500–600mAh/g [28].

The microstructure and composition of the LiF–Co nanocomposite with a highly heterogeneous mixture has been controlled by the pulsed laser deposition method on atomic or nanometer scale and presents an active electrochemical behavior. Subsequent charge/discharge processes still keep similar discharge/charge curves as the second one, with the cell exhibiting good stability, and a capacity fade of less than 0.3% per cycle after 65 charge–discharge cycles, indicating a highly active Co–LiF nanocomposite thin film with high specific capacities and good coulombic efficiency [29].
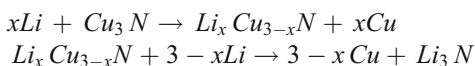
Nitrides

Ternary lithium transition metal nitrides have also been reported as negative electrode materials for secondary lithium batteries. The $Li_{2n-1}MN_n$ nitrides, such as Li_3FeN_2 [30] and Li_7MnN_4 [31], crystallize in structures derived from the cubic antifluorite, while the $Li_{3-x}M_xN$ nitrides [32–

35] where M is a transition metal such as Co, Ni, and Cu, are isostructural to the hexagonal layered Li_3N. The transition metal substitutes for Li between the Li_2N layers. In these materials, Li ions must be removed to reversibly react with lithium. The best candidate exhibiting good cycling stability and large capacity is $Li_{2.6}Co_{0.4}N$ with 700mAh/g. Some nitrides such as silicon tin oxynitride [36, 37], Sn_3N_4, [36, 38], and InN [38] have been reported to undergo, upon reaction with Li, an irreversible conversion reaction, generating a Li_3N [39–43] matrix as follows:

$$M_xN_y + 3yLi^+ + 3ye^- \quad \rightarrow \quad xM + yLi_3N$$

LiZnN has been isolated by way of an electrochemical conversion reaction of Zn_3N_2 with Li. Zn_3N_2 reversibly reacts with lithium electrochemically, exhibiting a large reduction capacity of 1,325mAh/g corresponding to the insertion of 3.7 Li per Zn. Of this initial capacity, 555mAh/g was found to be reversible. The reaction mechanism with lithium was identified as a conversion reaction of Zn_3N_2 into LiZn and a matrix of βLi_3N, the high pressure form of Li_3N. Upon oxidation, LiZn transformed into metallic Zn, while βLi_3N contributed to the transformation into LiZnN. The formation of LiZnN as the new end member of the electrochemical reaction with lithium was identified as the cause of the irreversible loss observed during the first cycle. The βLi_3N and LiZn oxidation into LiZnN was found to be reversible upon subsequent cycles. Poor cycle life was mainly attributed to the electromechanical grinding of the Li–Zn alloying reaction [44].

Pereira N et al. [45] reported the electrochemical reactivity of Cu_3N with lithium by conversion reaction. The reaction of Cu_3N with Li involved a three-step reaction mechanism in the first cycle—(1) the initial lithium intercalation into the open structure of Cu_3N, (2) the conversion of copper nitride into a Cu metal and Li_3N nanocomposite, and (3) the formation of an electrolyte interface layer at the surface of the nanocomposite. The latter two processes were found to be reversible. Cu_3N electrodes exhibited outstanding cycling efficiency at high rate (equivalent to 1.67 C). Although the copper nitride conversion process was found to be poor, extended cycling seemed to promote the development of electrochemical processes above 2V during delithiation. These seem to be associated with the formation during delithiation of Cu_2O and CuO due to electrolyte degradation.

$$xLi + Cu_3N \rightarrow Li_xCu_{3-x}N + xCu$$
$$Li_xCu_{3-x}N + 3 - xLi \rightarrow 3 - xCu + Li_3N$$

Sulfides

While most people thought of sulfides as lithium primary cell materials [46–49], some researchers showed in the 1970s that layered phases such as TiS_2 and MoS_2 were candidates as positive electrode materials for rechargeable lithium batteries [50, 51].

Recently, the conversion reactions are reported for sulfides of transition metals like cobalt and nickel. Unlike the oxides, the irreversible capacity during the first cycle is only of 14% (0.35 Li) as compared to about 25% for the oxides [52]. Such difference is nested in both a better ionic conductivity of Li_2S as compared to Li_2O and a better electronic conductivity of sulfides as compared to oxides. But, unfortunately, the irreversibility advantage of sulfides over the oxides during the first cycle does not hold upon subsequent cycles. For the sulfides, the capacity rapidly drops when increasing the number of cycles, and this drop is more pronounced for the Li/CuS cells as compared to the Li/NiS ones, while Li half-cells based on oxides (CoO for instance) maintain extremely well their reversibility upon cycling. Such a difference between oxides and sulfides in terms of capacity retention is rooted, in the partial solubility of Li_2S, into the electrolyte and not of Li_2O.

The Co and Ni sulfides react towards Li through conversion reactions, like their homologous oxides (CoO, NiO), leading during cell discharge to the appearance of metallic nanoparticles dispersed into a Li_2S matrix that convert back to nanoparticles of sulfides upon the following charge. CuS was shown to behave differently. Upon reduction, there is first the formation of an intermediate $Cu_{2-x}S$ phase that undergoes a displacement rather than a conversion reaction, leading to the formation of large copper dendrites surrounding a Li_2S matrix. During the following oxidation, dendrites disappear, and the copper reenters the matrix to recreate massive particles of $Cu_{2-x}S$ then CuS.

Nevertheless, whatever conversion or displacement reactions, sulfide phases suffer from cyclability issues owing to Li_2S solubility issues. To circumvent these issues, one can limit the cycling discharge cutoff voltage so as to operate within a potential range not permitting the Li_2S formation or search for the Li-based electrolyte that does not solvate Li_2S [52].

Antimonides

The electrochemical characterization of $NiSb_2$ versus Li^+/Li^0 shows a reversible uptake of five lithium per formula unit, which leads to reversible capacities of 500mAh/g at an average potential of 0.9V. During the first discharge, the orthorhombic $NiSb_2$ phase undergoes a pure conversion process ($NiSb_2 + 6 Li^+ + 6e^- \rightarrow Ni^0 + 2Li_3Sb$). During the charge process that follows, the lithium extraction from the composite electrode takes place through an original conversion process, leading to the formation of the high pressure $NiSb_2$ polymorph. This highly reversible mechanism makes

it possible to sustain 100% of the specific capacity after 15 cycles. For this compound, the cycling rate does not appear to be a kinetic limitation, as the performances are improved with increasing the cycling rate [53].

Ionica et al. [54] reported that MnSb reacted with lithium to form LiMnSb during discharge process. Further lithiation results in the formation of Li_3Sb. During the subsequent charge, the reactions are reversible; on fully charged, MnSb is regenerated, and the presence of LiMnSb phase was observed. The reversible capacity of these materials is of about 320–400mAh/g.

Tarascon et al. [55] reported the electrochemical reactivity of $CoSb_3$ vs. lithium. This phase reacts with more than 9.5 lithium in a two-step process, consisting of the uptake of nine Li at a constant voltage close to 0.6V and of about one lithium over the final voltage decay to 0.01V. Upon recharge, only eight lithium can be extracted. The constant voltage process is rooted in the decomposition of CoSb3, leading to the formation of a composite made of Co and Li_3Sb nanograins.

Ni Sb_2O_6 and $CoSb_2O_6$ showed similar electrochemical behavior, with an uptake of about 18–19 Li per formula unit along the first reduction and only six to seven Li reversibly removed upon subsequent cycling. This totally differs from the behavior of Cu Sb_2O_6 that was found to react with only about seven Li during the first reduction without any capacity recovered on subsequent charge. The reduced $CoSb_2O_6$ consists of 10–50nm Co particles dispersed in a $Li_3Sb + Li_2O$ matrix. For $CuSb_2O_6$, a two-step reduction occurs: first, the formation of Cu clusters through an electrochemically driven exchange reaction leading to $Li_2Sb_2^VO_6$ and then reduction of this matrix into 5-nm Sb domains dispersed in an insulating amorphous Li-rich $Li–Sb^V–O$ matrix, preventing any further alloying reaction and any charge reaction [56].

Phosphides

The low atomic weight and high availability of phosphorous allows us to expect larger gravimetric capacities than antimony-based electrodes and cheaper production. The transition metal compounds of Group V, such as nitrides [57] and antimonides [58], show a lower intercalation potential compared to the respective oxides. This results from the lower formal oxidation state of the metal and strong covalent character of the M–P and M–N bond, leading to high lying mixed anion-metal bands and a high degree of electron delocalization [59]. Although various transition metal compounds in Group V (nitrides and antimonides) have been reported to act as low potential Li insertion hosts, the phosphides have remained unexplored to date [60–66].

Pralong et al. showed that lithium uptake and extraction in the metal phosphide, CoP_3, provides a reversible capacity of 400mAh/g at an average potential of 0.9V vs.

Li/Li^+ via a novel mechanism. Initial uptake of Li forms highly dispersed cobalt clusters embedded in a matrix of Li_3P; extraction of Li from this ion-conductive matrix on charge yields nanoparticles of LiP, with little change evident in the oxidation state of the Co site. This shows that contrary to the case of metal oxides, here, the anion plays the major role in reduction and oxidation. Alcantara reported the reversible electrochemical reactivity of CoP_3 with lithium [60].

Monoclinic NiP_2 can reversibly uptake five lithium per formula unit, leading to reversible capacities of 1,000mAh/g at an average potential of 0.9V vs $Li^+/Li°$. During the first discharge, the cubic phase undergoes a pure conversion process as opposed to a sequential insertion-conversion process for monoclinic NiP_2 [64].

Tarascon et al. developed a novel design for NiP_2 electrodes that consists in growing the monoclinic NiP_2 phase through a vapor-phase transport process on a commercial Ni foam commonly used in Ni-based alkaline batteries. These new self-supported electrodes, based on chemically made interfaces, offer new opportunities to fully exploit the capacity gains provided by conversion reactions [61].

The amorphous sample of VP_2 can reversibly react with 3.5 Li per formula unit as compared to solely 2.5 for the crystalline one [65].

The electrochemical reactivity toward lithium of various Zn_3P_2 powders is shown to be unique despite some quantitative performance differences. The insertion mechanism is shown to involve two distinct but parallel reversible pathways for a large number of inserted lithium (up to nine): one implies exclusively phosphide phases: Zn_3P_2, LiZnP, Li_4ZnP_2, and Li_3P [66]. The second one involves only Li–Zn alloys: Zn, $LiZn_4$, and LiZn [63].

Conclusion

A brief review on electrode materials which undergo conversion reactions involving more than one electron per 3D metal is presented. It is clear from the above review that the realization of improved energy is possible by adapting to newer reaction pathways than the conventional insertion and de-insertion reaction. This will open newer unconventional areas to maximize the energy output which will lead to the electronic revolution with a lot of applications.

References

1. Idota Y, Maekawa TKA, Miyasaka T (1997) Science 276:1395
2. Tarascon J-M, Armand M (2001) Nature 414(6861):359
3. Leroux F, Power GROWP, Nazar LF (1998) Electrochem Solid State Lett 1(6):255

4. Hu J, Li H, Huang X (2005) Electrochem Solid State Lett 8:A66
5. Pralong V, Leriche J-B, Beaudoin B, Naudin E, Morcrette M, Tarascon J-M (2004) Solid State Ion 166(3):295
6. D'ebart A, Dupont L, Poizot P, Leriche J-B, Tarascon J-M (2001) J Electrochem Soc 148:A1266
7. Dupont L, Grugeon S, Laruelle S, Tarascon J-M (2007) J Power Sources 164(2):839–848
8. Taberna PL, Mitra S, Poizot P, Simon P, Tarascon J-M (2006) Nat Mater 5:567–573
9. Poizot P, Laruelle S, Grugeon S, Dupont L, Tarascon J-M (2000) Nature 407:496
10. Li W-Y, Xu L-N, Chen J (2005) Adv Funct Mater 15:851–857
11. Wang Y, Yang C-M, Schmidt W, Spliethoff B, Bill E, Schuth F (2005) Adv Mater 17:53–56
12. Kleitz F, Choi SH, Ryoo R (2003) Chem Commun 17:2136–2137
13. Tian BZ, Liu XY, Solovyov LA, Liu Z, Yang HF, Zhang ZD, Xie SH, Zhang FQ, Tu B, Yu CZ, Terasaki O, Zhao DY (2004) J Am Chem Soc 126:865–875
14. Zhao DY, Feng JL, Huo QS, Melosh N, Fredrickson GH, Chmelka BF, Stucky GD (1998) Science 279:548–552
15. Jiao F, Shaju KM, Bruce PG (2005) Angew Chem Int Ed 44:6550–6553
16. Larcher D, Sudant G, Leriche J-B, Chabre Y, Tarascon J-M (2002) J Electrochem Soc 149(3):A234–A241
17. Thackeray MM, Backer SD, Adendorff KT (1985) Solid State Ion 17:175
18. Laruelle S, Grugeon S, Poizot P, Dolle M, Dupont L, Tarascon J-M (2002) J Electrochem Soc 149:A627–A634
19. Yuan Z, Huang F, Feng C, Sun J, Zhou Y (2003) Mater Chem Phys 79:1–4
20. Shaju KM, Jiao F, De'bart A, Bruce PG (2007) Phys Chem Chem Phys 9(15):1837–1842
21. Jiao F, Bao J, Bruce PG (2007) Electrochem Solid State Lett 10 (12):A264–A266
22. Balaya P, Li H, Kienle L, Maier J (2003) Adv Funct Mater 13:621
23. Maier J (2005) Nat Mater 4:805
24. Balaya P, Li H, Kienle L, Maier J (2003) Adv Funct Mater 13 (8):621–625
25. Dupont L, Laruelle S, Grugeon S, Dickinson C, Zhoub W, Tarascon J-M (2008) J Power Sources 175:502–509
26. Grugeon S, Laruelle S, Dupont L, Chevallier F, Taberna PL, Simon P, Gireaud L, Lascaud S, Vidal E, Yrieix B, Tarascon J-M (2005) Chem Mater 17(20):5041–5047
27. Badway F, Cosandey F, Pereira N, Amatucci GG (2003) J Electrochem Soc 150(10):A1318–A1327
28. Li H, Richter G, Maier J (2003) Adv Mater 9:15
29. Zhou Y, Liu W, Xue M, Yu L, Wu C, Wu X, Fu Z (2006) Electrochem Solid State Lett 9(3):A147–A150
30. Nishijima M, Takeda Y, Imanishi N, Yamamoto O (1994) J Solid State Chem 113:205
31. Nishijima M, Tadokoro N, Takeda Y, Imanishi N, Yamamoto O (1994) J Electrochem Soc 141:2966
32. Nishijima M, Kagohashi T, Imanishi N, Takeda Y, Yamamoto O, Kondo S (1996) Solid State Ion 83:107
33. Shodai T, Okada S, Tobishima S, Yamaki J (1996) Solid State Ion 86–88:785
34. Shodai T, Okada S, Tobishima S, Yamaki J (1997) J Power Sources 68:515
35. Takeda Y, Nishijima M, Yamahata M, Takeda K, Imanishi N, Yamamoto O (2000) Solid State Ion 130:61
36. Bates JB, Dudney NJ, Neudecker B, Ueda A, Evans CD (2000) Solid State Ion 135:33
37. Neudecker BJ, Zuhr RA, Bates JB (1999) J Power Sources 81–82:27
38. Neudecker BJ, Zuhr RA (2000) In: Nazri G-A, Thockeray M, Ohzuku T (eds) Intercalation compounds for battery materials PV 99–24. The Electrochemical Society Proceedings Series, Pennington, NJ, p 295
39. Boukamp BA, Huggins RA (1978) Mater Res Bull 13:23
40. Rea JR, Foster DL (1979) Mater Res Bull 14:841
41. Rabenau A (1982) Solid State Ion 6:277
42. Lapp T, Skaarup S (1983) Solid State Ion 11:97
43. Richard PM (1980) J Solid State Chem 33:127
44. Pereira N, Klein LC, Amatucci GG (2002) J Electrochem Soc 149 (3):A262–A271
45. Pereira N, Dupont L, Tarascon JM, Klein CLC, Amatucci GG (2003) J Electrochem Soc 150(9):A1273–A1280
46. SAFT (1966) French Patent 1(490):725
47. Gabano JP, Dechenaux V, Gerbier G, Jammet J (1972) J Electrochem Soc 114:459
48. Jasinski R, Burrows B (1969) J Electrochem Soc 116:422
49. Linden D (1995) Handbook of batteries. McGraw-Hill, New York
50. Armand M (1973) In: Van Goll W (ed) New electrode materials in fast ion transport in solids. North Holland, Amsterdam
51. Steele BCH (1973) In: Van Goll W (ed) Chemical diffusion in fast ion transport in solids. North Holland, Amsterdam
52. Dupont DL, Patrice R, Tarascon J-M (2006) Solid State Sci 8:640–651
53. Villevieille C, Ionica-Bousquet C-M, Ducourant B, Jumas J-C, Monconduit L (2007) J Power Sources 172:388–394
54. Ionica CM, Lippens PE, Fourcade JO, Jumas J-C (2005) J Power Sources 146:478–481
55. Tarascon J-M, Morcrette M, Dupont L, Chabre Y, Payen C, Larcher D, Pralonga V (2003) J Electrochem Soc 150(6):A732–A741
56. Larcher D, Prakash AS, Laffont L, Womes M, Jumas JC, Olivier-Fourcade J, Hedge MS, Tarascon J-M (2006) J Electrochem Soc 153(9):A1778–A1787
57. Nishijima M, Kagohashi T, Imanishi M, Takeda Y, Yamamoto O, Kondo S (1996) Solid State Ion 83:107
58. Shodai T, Okada S, Tobishima S, Yamaki J (1996) J Solid State Ion 86–88:785
59. Takeda Y, Nishijima M, Yamahata M, Takeda K, Imanishi N, Yamamoto O (2000) Solid State Ion 130:61
60. Alcantara R, Fernandez-Madrigal FJ, Lavela P, Tirado JL, Jumas J-C, Olivier-Fourcade J (1999) J Mater Chem 9:2517
61. Lefebvre-Devos M, Lassalle M, Wallart X, Olivier-Fourcade J, Monconduit L, Jumas J-C (2001) Phys Rev B 63:125110
62. Monconduit L, Tillard-Charbonnel M, Belin C (2001) J Solid State Chem 156:37
63. Pralong V, Souza DCS, Leung KT, Nazar LF (2002) Electrochem Commun 4:516–520
64. Gillot F, Boyanov S, Dupont L, Doublet M-L, Morcrette M, Monconduit L, Tarascon J-M (2005) Chem Mater 17:6327–6337
65. Gillot F, M'en'etrier M, Bekaert E, Dupont L, Morcrette M, Monconduit L, Tarascon JM (2007) J Power Sources 172:877–885
66. Bichat M-P, Pascal J-L, Gillot F, Favier F (2005) Chem Mater 17:6761–6771